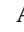




Physical properties of $(\text{Mn}_{1-x}\text{Co}_x)\text{Si}$ at $x \simeq 0.060\text{--}0.100$: Quantum criticalityA. E. Petrova , S. Yu. Gavrilkin, and G. V. Rybalchenko
*P. N. Lebedev Physical Institute, Leninsky pr., 53, 119991 Moscow, Russia*Dirk Menzel
*Institut für Physik der Kondensierten Materie, Technische Universität Braunschweig, D-38106 Braunschweig, Germany*I. P. Zibrov 
*Institute for High Pressure Physics of RAS, 108840 Troitsk, Russia*S. M. Stishov *
P. N. Lebedev Physical Institute, Leninsky pr., 53, 119991 Moscow, Russia (Received 12 November 2020; revised 10 March 2021; accepted 19 April 2021; published 3 May 2021)

We have grown and characterized three samples of Co-doped MnSi and studied their physical properties (magnetization and magnetic susceptibility, heat capacity, and electrical resistance). All three samples show non-Fermi liquid physical properties. From literature data and current results it follows that impurities (Co and Fe) eliminate the first-order phase transition peaks and spread the fluctuation maxima in such a way that the low-temperature part effectively reaches the zero temperature, where the fluctuations inevitably become quantum. The behavior of low-temperature parts of the heat capacity of the samples suggests that a gradual transition from classical to quantum fluctuations can be described by a simple power function of temperature with the exponent less than one. The $d\rho/dT$ data generally support this suggestion. The values of the heat capacity exponents immediately lead to the diverging ratio C_p/T and hence to the diverging effective electron mass. We found that at a large concentration of the dopant there are no distinct phase transition points. What we observe is probably a region of the helical fluctuations spreading over a significant range of concentrations and temperatures, which become quantum close to 0 K.

DOI: [10.1103/PhysRevB.103.L180401](https://doi.org/10.1103/PhysRevB.103.L180401)**I. INTRODUCTION**

In recent years the quantum critical phenomena in magnetic systems have attracted much attention. In the course of intensive studies, the helical magnet MnSi has played a special role as a material available in an almost perfect single-crystal form, whose phase diagram and physical properties at high pressure were well known. As was shown in many studies the magnetic phase transition point in MnSi decreases with pressure and reaches almost zero at about 1.4 GPa [1–3]. At the same time no evidence for quantum critical behavior was seen in MnSi at high pressure [4–6]. One of the reasons for this situation could be strong nonhydrostatic stress developing at high compression [5–7]. To avoid this complication, it is reasonable to try using so-called “chemical” pressure, which is replacing some atoms or ions of the material with chemically suitable atoms of smaller size. This procedure normally results in a volume decrease, which could imitate a high-pressure effect. Of course, it causes a certain disorder in materials that should be taken into account in the data interpretation. The described idea was used at studying the iron- and cobalt-doped MnSi in Refs. [8–10]. As was shown

in Refs. [9,10] the iron-doped sample of MnSi with a nominal composition $\text{Mn}_{0.85}\text{Fe}_{0.15}\text{Si}$ reveals features inherited to the proximity of quantum critical point. However, the results for Co-doped samples, obtained in Ref. [9], were not quite conclusive.

So, with all that in mind, we decided to extend the study [9] in relation to Co-doped samples of MnSi.

II. EXPERIMENTAL

We prepared three samples with the nominal composition: $\text{Mn}_{0.94}\text{Co}_{0.06}\text{Si}$, $\text{Mn}_{0.92}\text{Co}_{0.08}\text{Si}$, $\text{Mn}_{0.9}\text{Co}_{0.1}\text{Si}$. Polycrystalline ingots containing Mn (Chempur; purity 99.99%), Co (Chempur; purity 99.95%), and Si ($\rho_n = 300 \text{ Ohm cm}$, $\rho_p = 3000 \text{ Ohm cm}$) were prepared by arc melting under argon atmosphere. Afterwards, single crystals have been grown using the triarc Czochralski technique.

The electron-probe microanalysis shows that real compositions are $\text{Mn}_{0.93}\text{Co}_{0.057}\text{Si}$, $\text{Mn}_{0.92}\text{Co}_{0.063}\text{Si}$, $\text{Mn}_{0.89}\text{Co}_{0.09}\text{Si}$, which indicates that two first samples have practically identical compositions despite the initial concentration of doping element (Table I). As was claimed in Ref. [11] the spin glasses form in $\text{Mn}_{1-x}\text{Co}_x\text{Si}$ at $x < 0.05 < 0.9$, which covers the concentration range indicated above. However, we could not find any distinct proofs for a spin glass behavior in the current

*stishovsm@lebedev.ru

TABLE I. Chemical compositions and lattice parameters of (Mn, Co)Si, (Mn, Fe)Si, and MnSi samples. a -lattice parameter, V -unit cell volume.

Nominal composition	Electron-probe composition	a Å	V Å ³
Mn _{0.94} Co _{0.06}	Mn _{0.93} Co _{0.057} Si ^a	4.5522	94.333
Mn _{0.92} Co _{0.08} Si	Mn _{0.92} Co _{0.063} Si ^a	4.5519	94.313
Mn _{0.9} Co _{0.1} Si	Mn _{0.89} Co _{0.09} Si ^a	4.5499	94.189
Mn _{0.85} Fe _{0.15} Si	Mn _{0.83} Fe _{0.17} Si ^b	4.5462	93.961
MnSi	MnSi ^c	4.5598	94.8063

^aCurrent paper.

^bRef. [10] (chemical composition data in the table obtained in new facilities are slightly different from Ref. [10]).

^cRef. [5].

experiments. So we believe that the itinerant nature of the materials is conserved.

We performed some magnetic, heat capacity, and resistivity measurements to characterize the (Mn, Co)Si samples. All measurements were made making use the Quantum Design PPMS system with the heat capacity and vibrating magnetometer moduli and the He-3 Refrigerator. The resistivity data were obtained with the standard four-terminals scheme using the spark-welded Pt wires as electrical contacts.

The experimental data are shown in Figs. 1–9.

Figure 1 illustrates magnetization of the samples in the fields to 9 T. As is seen there are no indications for spontaneous magnetic moments in these materials.

The magnetic susceptibility of (Mn, Co)Si samples is demonstrated in Fig. 2 in the limited range of temperature for a better view of the specific features of these curves. At first sight these features are nothing other than strongly deformed maximum of $\chi(T)$ observed in the pure MnSi at the phase transition point (see Fig. 2). Similar maxima in $\chi(T)$ were seen in [9] at lower Co concentrations. If these maxima indeed correspond to the “phase transition” points it worth comparing

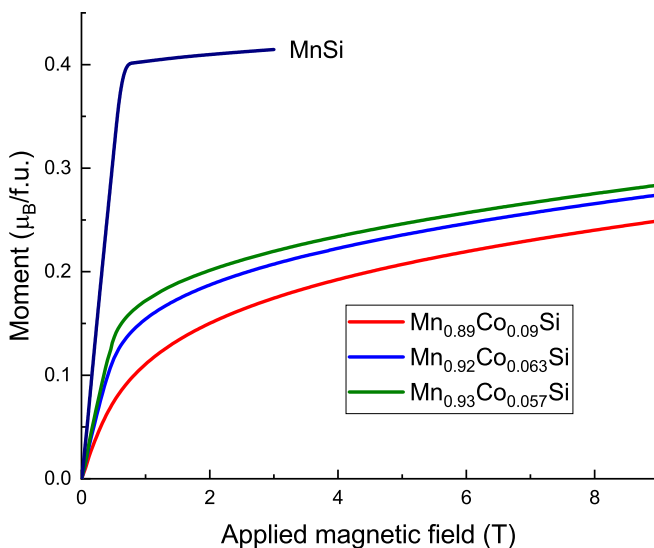


FIG. 1. Magnetizations of samples (Mn, Co)Si at 2 K. Data for MnSi are shown for comparison [5].

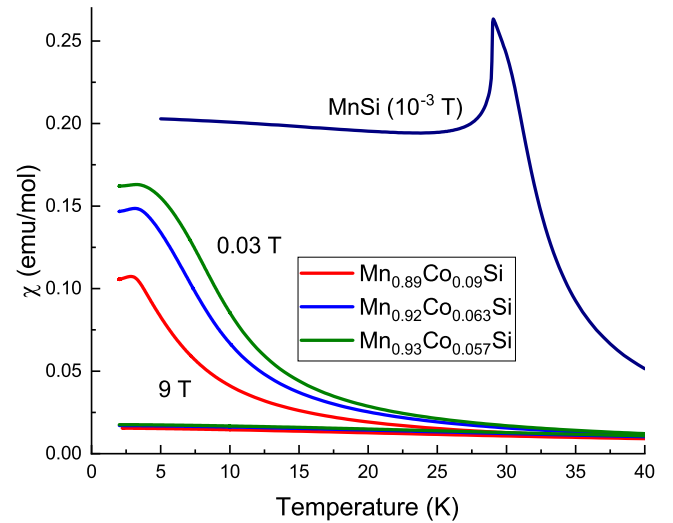


FIG. 2. Magnetic susceptibility of (Mn, Co)Si as a function of temperature at 0.03 and 9 T, Magnetic susceptibility of pure MnSi is shown as well [5].

the data with the results of Ref. [9], which will be done later in this paper.

The results of heat capacity measurements are displayed in Fig. 3. As is seen in Fig. 4 the lines of $C_p(T)$ changes their slope rather sharply at temperatures in the vicinity of 4–5 K. These features can be attributed to the strongly smeared out the fluctuation-induced heat capacity maximum associated with the magnetic phase transition in pure MnSi.

The mentioned slope change, which becomes more evident after subtraction from the heat capacity curve at zero magnetic field the corresponding curve at 9 T, occurs

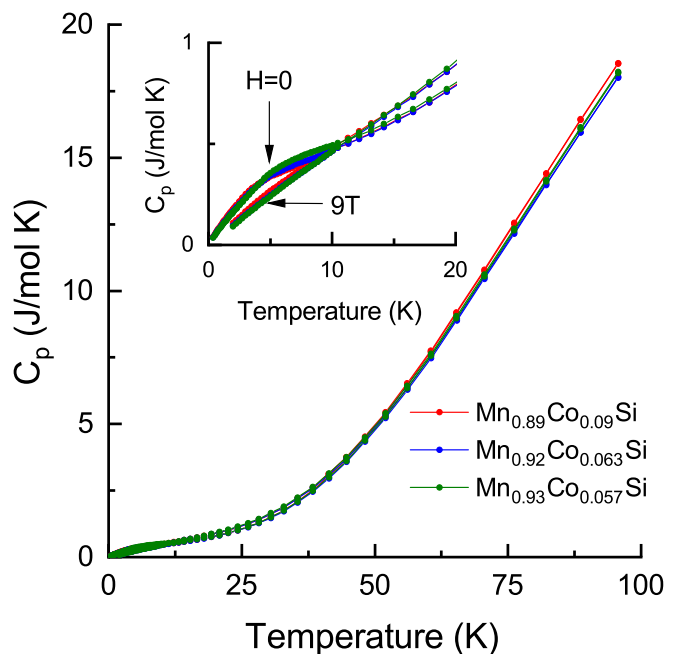


FIG. 3. Heat capacity of (Mn, Co)Si at zero and 9 T as a function of temperature in the range 0.4–100 K. Enlarged part of the plot is in the inset.

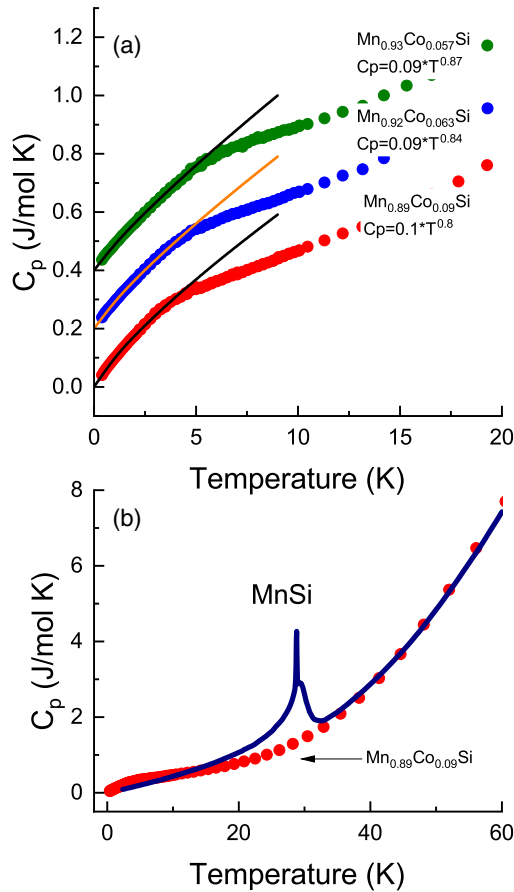


FIG. 4. (a) Illustration of the fitting of the low-temperature part of heat capacity to the power function. The values of the power exponents are shown in the plot. The data are shown with offsets for better viewing. (b) Heat capacity of pure MnSi [5] in comparison with a Co-doped sample.

at ~ 5 K ($\text{Mn}_{0.93}\text{Co}_{0.057}\text{Si}$), ~ 4.7 K ($\text{Mn}_{0.92}\text{Co}_{0.063}\text{Si}$), and ~ 3.4 K ($\text{Mn}_{0.89}\text{Co}_{0.09}\text{Si}$) (Fig. 5). This manipulation implies a subtraction of some background contributions, including phonon and electron ones to the heat capacity leaving the spin fluctuation part intact. Indeed, a strong magnetic field suppresses the spin fluctuations and not significantly influences the phonon and electron heat capacity [12]. At the same time as seen in Fig. 5 this procedure reduces the low-temperature parts of the C_p to the puzzling universal line even including data on MnFeSi [10]. On the other hand, the high-temperature parts of the differential C_p curves became negative at some temperatures, therefore supporting our old conclusion that strong fluctuations give negative contributions to the heat capacity of the paramagnetic phase of MnSi [13].

The maximum temperatures of the curves in Fig. 5 generally correlate with the local maxima of $\chi(T)$ taken as the “phase transition” temperatures (see Fig. 2). In Fig. 6 it is seen that data points with concentration $x \approx 0.06$ fit well with data of Ref. [9], whereas the ones with $x = 0.09$ sharply deviate from the suggested curve. Moreover, as seen in Fig. 6 the “phase transition” temperature somehow avoids declining at further increase of the Co concentration. If this feature may

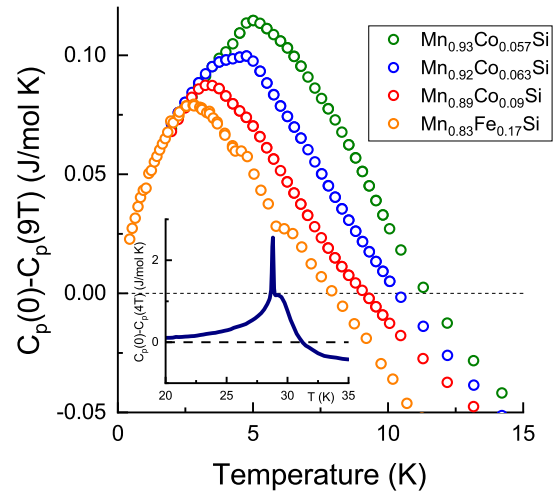


FIG. 5. The difference between heat capacity at zero magnetic field $C_p(0)$ and heat capacity at 9 T ($C_p(9T)$) for (Mn, Co)Si samples (current work) and one sample of (Mn, Fe)Si [10]. In the inset corresponding data for pure MnSi are shown. As seen the Co doping destroys the first-order phase transition peak, spreads out fluctuation maxima, and shifts maxima to lower temperatures.

indicate the spin glass revelation remains to be seen at a larger concentration of the dopant.

The low-temperature parts of the heat capacity curves reflect a gradual transition from classical to quantum fluctuations, which can be described by a simple power function of temperature with the exponent less than one. The latter immediately leads to the diverging ratio C_p/T (see Fig. 7)

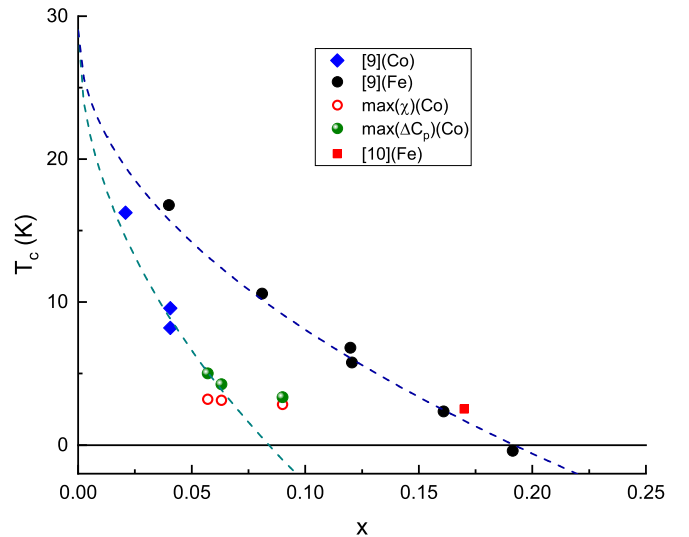


FIG. 6. “Phase transition” temperature as a function of concentrations for $\text{Mn}_{1-x}\text{Fe}_x\text{Si}$ [9,10] and $\text{Mn}_{1-x}\text{Co}_x\text{Si}$ [9] and current data. Nature of dopants is indicated in the legend. In Ref. [9] “phase transition” temperatures were determined from the temperature dependence of magnetic moments. Current data were taken as the χ maxima (Fig. 2) and maxima of $\Delta C_p(0 - 9T)$ (Fig. 5). Note that the square data point on the “iron” curve corresponds to the sample studied in [10]. [Corrected composition was used. Transition temperature was taken as a maximum of $\Delta C_p(0 - 9T)$ (Fig. 5).]

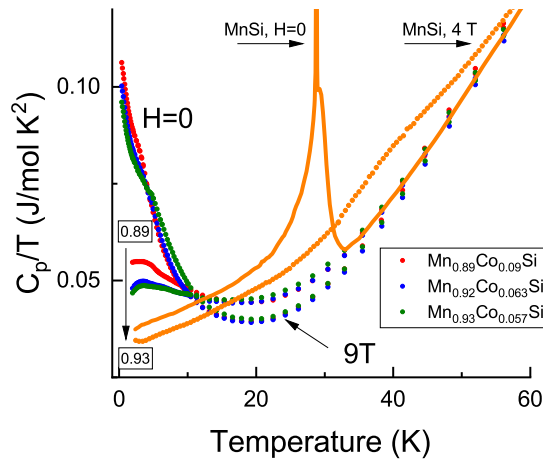


FIG. 7. The ratio C_p/T for (Mn,Co) samples as a function of temperature at zero and 9 T magnetic fields. It is seen that diverging of C_p/T is suppressed by strong magnetic field. The C_p/T data for MnSi are shown for comparison [5].

and hence to the diverging effective electron mass, which is a signature of the quantum critical behavior.

The resistivity of the samples as a function of temperature exhibits an evolution from the low-temperature region of not quite clear underlying physics to the “saturation” regime typical of the strongly disordered metals [14] (Fig. 8; see also Ref. [10]).

Figure 8 illustrates this kind of the resistivity behavior in magnetic field to 9 T using the sample $\text{Mn}_{0.89}\text{Co}_{0.09}\text{Si}$ as a typical example. In an attempt to understand the low-temperature conduct of the resistivity we performed a fitting of the corresponding data with the expression $\rho = A + BT^n$ in the range 2–8 K. The following values of exponents n were ob-

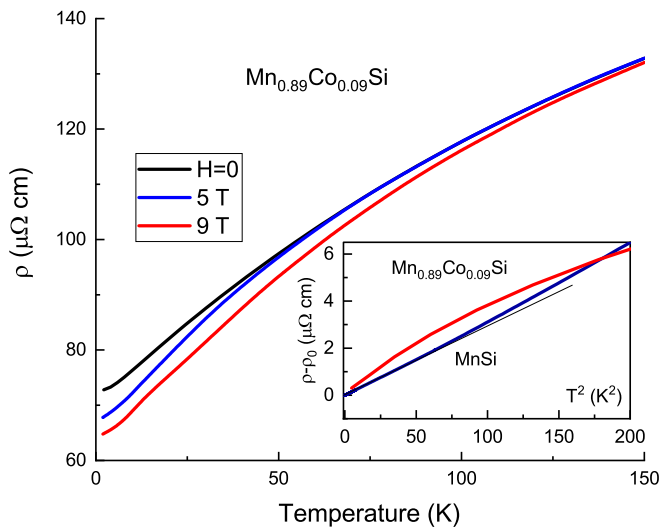


FIG. 8. The dependence of resistivity of $\text{Mn}_{0.89}\text{Co}_{0.09}\text{Si}$ on temperature at various magnetic fields. In the inset resistivity of $\text{Mn}_{0.89}\text{Co}_{0.09}\text{Si}$ and pure MnSi [17] as functions of T^2 is shown at zero magnetic field. The Fermi-liquid feature is evident in MnSi at temperature up to 10 K. Otherwise the doped sample reveals the non-Fermi liquid behavior.

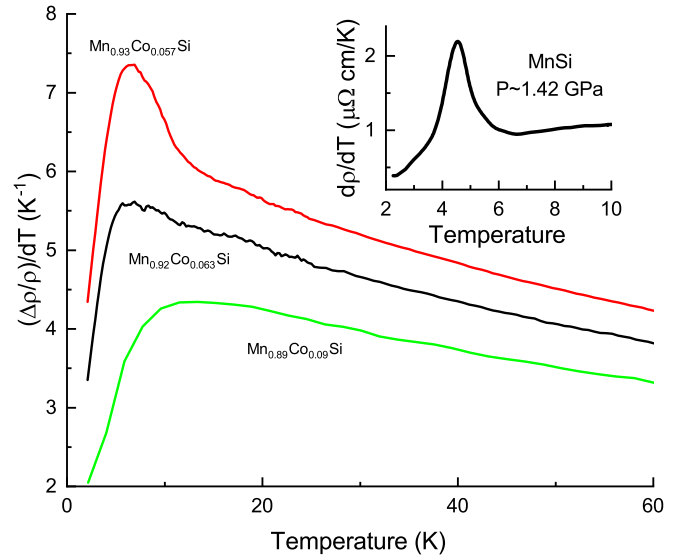


FIG. 9. Temperature derivatives of resistivity of the samples $\text{Mn}_{1-x}\text{Co}_x\text{Si}$. In the inset $d\rho/dT$ data [6] for pure MnSi at the phase transition occurring at high pressure and at the appropriate temperature range are shown for comparison purpose.

tained: $n = 1.7$ ($H = 0$), $n = 1.4$ ($5 T$), $n = 1.6$ ($9 T$), which uncovers non-Fermi-liquid behavior (see [15,16]). The inset in Fig. 8 illustrates this situation.

Temperature derivatives of resistivity of the samples $\text{Mn}_{1-x}\text{Co}_x\text{Si}$ are displayed in Fig. 9. These data correlate in certain aspects with those shown in Figs. 4 and 5 identifying the low-temperature parts of the corresponding curves with the smeared-out low-temperature sides of the fluctuation maxima (see the inset where $d\rho/dT$ data for the high-pressure phase transition in pure MnSi are demonstrated).

III. DISCUSSION

As can be seen in Figs. 4, 5, and 7 the phase transition in pure MnSi is characterized by a sharp peak on top of a rounded maximum forming a shoulder in the

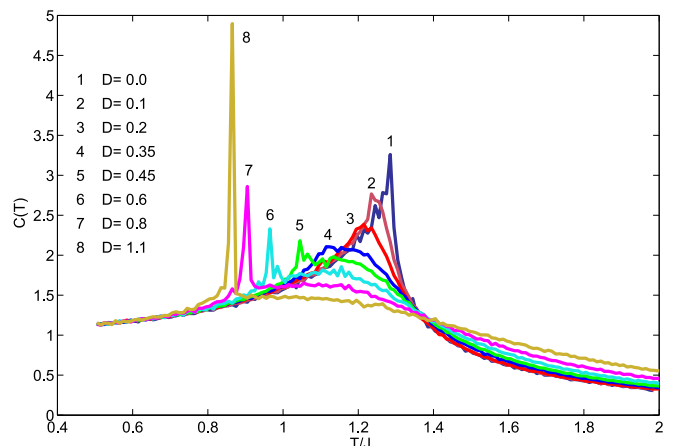


FIG. 10. Temperature dependence of the specific heat $C(T)$ for the Hamiltonian $H = H_J + H_D$ for different values of the DM (D) interaction (after Ref. [18]).

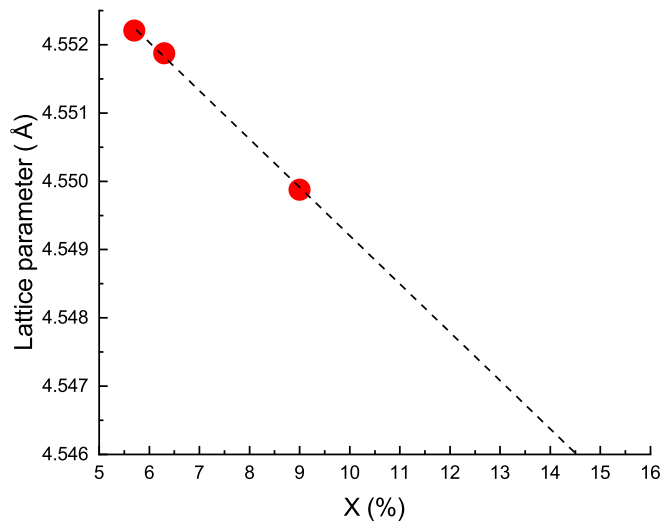


FIG. 11. Lattice parameter of $\text{Mn}_{1-x}\text{Co}_x\text{Si}$ as a function of Co concentration (X) (Table I).

high-temperature side of the peak. According to the Monte Carlo calculations [18] such structure of the heat capacity results from the perturbation of a virtual second-order ferromagnetic phase transition by the helical fluctuations, which smear out the transition and eventually condense into the helically ordered phase by a weak first-order phase transition (see Fig. 10). It is important to emphasize that the mentioned rounded maximum arises as a result of powerful helical spin fluctuations as was shown in a number of studies (see [19–21]).

From the data [9] and the current results follow that impurities (Co and Fe) destroy the first-order peaks, shift the fluctuation maxima to lower temperatures, and spread the maxima in such a way that its low-temperature part effectively reaches zero temperature, where the fluctuations inevitably become quantum (see Fig. 5). However, a doping action of Co obviously saturates at some concentrations, so the χ and $C_p(0) - C_p(9T)$ maxima do not move significantly with concentration increasing (Figs. 2 and 5). Nevertheless, we are unable to connect this feature with the spin glass formation as suggested in Ref. [11]. Note that in Ref. [10] the quantum critical trajectory was identified for the sample $\text{Mn}_{0.83}\text{Fe}_{0.17}\text{Si}$ with a lattice parameter 4.5462 Å; the value coincides with the lattice parameter of pure MnSi at the phase transition point at $T \sim 0$ K and $P \sim 14.5$ kbar (a quantum critical trajectory is a line, characterized by some constant parameter, in the given case concentration which reaches QCP at decreasing tem-

perature). Following this reasoning, we plot available lattice parameter data of (Mn, Co)Si as a function of Co concentration (Fig. 11). The extrapolation by Vegard's rule shows that the value of the lattice parameter equal to 4.5462 Å for (Mn, Co)Si can be attained at 14%–15% concentration of Co, i.e., at composition $\text{Mn}_{0.85}\text{Co}_{0.14-0.15}\text{Si}$. However, it is not clear whether this concentration is reachable. Moreover, in the light of the current study one hardly can find a unique single critical trajectory. Probably the same should be applicable to the $\text{Mn}_{1-x}\text{Fe}_x\text{Si}$ case. So the conclusion of Ref. [10] may be need a modification.

Thus, at present concentrations of the dopant there is not a definite phase transition point; instead one has a region of the helical fluctuations, which spread over a significant range of concentrations and temperatures and become quantum close to 0 K. Diverging the ratio C_p/T justifies this fact and leads to infinite electronic effective mass as a signature of quantum criticality (Fig. 7).

IV. CONCLUSION

We have grown and characterized three samples of Co-doped MnSi and studied their physical properties (magnetization and magnetic susceptibility, heat capacity, and electrical resistance). All three samples show non-Fermi liquid physical properties. From the data [9] and current results follow that impurities (Co and Fe) eliminate the first-order phase transition peaks and spread the fluctuation maxima in such a way that the low-temperature part effectively reaches the zero temperature, where the fluctuations inevitably become quantum (see Figs. 4 and 5). The behavior of low-temperature parts of the heat capacity of the samples (Figs. 4 and 5) suggests that a gradual transition from classical to quantum fluctuations can be described by a simple power function of temperature with the exponent less than one. The $d\rho/dT$ data generally support this suggestion (Fig. 9). The value of the heat capacity exponents immediately leads to the diverging ratio C_p/T (see Fig. 7) and hence to the diverging effective electron mass. We found out that at large concentration of the dopant there are no distinct phase transition points (Figs. 2 and 5). What we observe is a region of the helical fluctuations spreading over a significant range of concentrations and temperatures, which become quantum close to 0 K (Fig. 6).

ACKNOWLEDGMENTS

The authors gratefully acknowledge the technical support of Dr. V. A. Sidorov. A.E.P. and S.M.S. greatly appreciate financial support of the Russian Science Foundation (Grant No. 17-12-01050P).

- [1] J. D. Thompson, Z. Fisk, and G. G. Lonzarich, *Physica B* **161**, 317 (1989).
- [2] C. Pfeleiderer, G. J. McMullan, and G. G. Lonzarich, *Physica B* **206–207**, 847 (1995).
- [3] C. Thessieu, J. Flouquet, G. Lapertot, A. N. Stepanov, and D. Jaccard, *Solid State Commun.* **95**, 707 (1995).

- [4] C. Pfeleiderer, P. Böni, T. Keller, U. K. Rößler, and A. Rosch, *Science* **316**, 1871 (2007).
- [5] S. M. Stishov and A. E. Petrova, *Phys. Usp.* **54**, 1117 (2011).
- [6] A. E. Petrova and S. M. Stishov, *Phys. Rev. B* **86**, 174407 (2012).
- [7] A. M. Belemuk and S. M. Stishov, *J. Phys.: Condens. Matter* **31**, 135801 (2019).

- [8] C. Meingast, Q. Zhang, T. Wolf, F. Hardy, K. Grube, W. Knafo, P. Adelmann, P. Schweiss, H. v. Löhneysen, V. Zlatić, and A. C. Hewson (Eds.), *Properties and Applications of Thermoelectric Materials*, NATO Science for Peace and Security Series B: Physics and Biophysics Vol. 261 (Springer Science-Business Media, New York, 2009).
- [9] A. Bauer, A. Neubauer, C. Franz, W. Münzer, M. Garst, and C. Pfleiderer, *Phys. Rev. B* **82**, 064404 (2010).
- [10] A. E. Petrova, S. Yu. Gavrilkin, D. Menzel, and S. M. Stishov, *Phys. Rev. B* **100**, 094403 (2019).
- [11] J. Teyssier, E. Giannini, V. Guritanu, R. Viennois, D. van der Marel, A. Amato, and S. N. Gvasaliya, *Phys. Rev. B* **82**, 064417 (2010).
- [12] S. M. Stishov, A. E. Petrova, S. Khasanov, G. Kh. Panova, A. A. Shikov, J. C. Lashley, D. Wu, and T. A. Lograsso, *J. Phys.: Condens. Matter* **20**, 235222 (2008).
- [13] S. M. Stishov, A. E. Petrova, A. A. Shikov, Th. A. Lograsso, E. I. Isaev, B. Johansson, and L. L. Daemen, *Phys. Rev. Lett.* **105**, 236403 (2010).
- [14] H. Wiesmann, M. Gurvitch, H. Lutz, A. Ghosh, B. Schwarz, M. Strongin, P. B. Allen, and J. W. Halley, *Phys. Rev. Lett.* **38**, 782 (1977).
- [15] G. R. Stewart, *Rev. Mod. Phys.* **73**, 797 (2001).
- [16] M. Brando, D. Belitz, F. M. Grosche, and T. R. Kirkpatrick, *Rev. Mod. Phys.* **88**, 025006 (2016).
- [17] A. E. Petrova, E. D. Bauer, V. Krasnorussky, and S. M. Stishov, *Phys. Rev. B* **74**, 092401 (2006).
- [18] A. M. Belemuk and S. M. Stishov, *Phys. Rev. B* **95**, 224433 (2017).
- [19] S. V. Grigoriev, S. V. Maleyev, A. I. Okorokov, Yu. O. Chetverikov, R. Georgii, P. Böni, D. Lamago, H. Eckerlebe, and K. Pranzas, *Phys. Rev. B* **72**, 134420 (2005).
- [20] C. Pappas, E. Lelievre-Berna, P. Bentley, P. Falus, P. Fouquet, and B. Farago, *Phys. Rev. B* **83**, 224405 (2011).
- [21] M. Janoschek, M. Garst, A. Bauer, P. Krautscheid, R. Georgii, P. Böni, and C. Pfleiderer, *Phys. Rev. B* **87**, 134407 (2013).